

Collective-variable approach to the dynamics of nonlinear magnetic excitations with application to vortices

A. R. Völkel,* G. M. Wysin,† F. G. Mertens,‡ A. R. Bishop, and H. J. Schnitzer‡

Theoretical Division, Los Alamos National Laboratory, MS B262, Los Alamos, New Mexico 87545

(Received 15 April 1994)

We propose a collective-variable ansatz for a system of N extended, but finite, nonlinear excitations in magnetic systems. In contrast to earlier approaches, where the interactions between the different excitations have been treated only through an external force term, we explicitly consider a dependence of the microscopic spin field on all the coordinates and velocities of the localized objects. This leads to N coupled equations of motion with parameters (mass and gyro tensors) which explicitly depend on the mutual distances of the excitations. We apply this ansatz to vortices in two-dimensional Heisenberg ferromagnets with weak easy-plane anisotropy. For vortex pairs we find either rotational or translational motion, with an additional cyclotronlike oscillation on top of the main trajectories. Due to the interactions between the two vortices we obtain two different eigenvalues of the mass and gyro tensors with values depending on the distance between the vortices, their vorticities, and the sign of their out-of-plane structures. In contrast to the single-vortex mass, which depends logarithmically on the system size L , we find two-vortex masses, which are independent of L , but depend on their mutual distance. These predictions are in good qualitative agreement with numerical simulations of the complete spin systems. However, since these simulations are performed at zero temperature, where the vortex pairs extend throughout the whole system, we observe a strong influence of the boundaries on the absolute values of the masses.

I. INTRODUCTION

Nonlinear excitations play an important role in many different areas of physics, which has led to an increasing interest in these objects in the last 30 years.^{1,2} Unfortunately, only a few nonlinear systems—most of them one dimensional (1D)—can be treated exactly. In general one has to develop approximate methods to understand the dynamics of these systems. For the case of well-localized nonlinear excitations *collective-variable* approaches have been proven quite successful for many applications.³ In these approaches, the nonlinear excitations are treated as particlelike structures (on a mesoscopic length scale) with well-defined positions and velocities. Even their interaction with the surrounding fluctuations can be incorporated to some degree.^{4,5}

Magnetic systems are particularly useful for studying nonlinear phenomena, because (i) they allow for many different nonlinear excitations, e.g., domain walls, vortices, bubbles, etc., depending on the form of the mutual interaction of the magnetic moments and with applied external fields; (ii) they can be mapped, at least in the 1D case, for some limiting cases onto completely integrable systems; (iii) they are relatively easy to simulate on computers, even for physically relevant system sizes, i.e., larger than the characteristic length scales of the quantities under investigation.

We will focus here on 2D magnetic systems which can show, due to their intermediate dimensionality, a quite genuine dynamical behavior.⁶ For example, Heisenberg magnets with XY - or easy-plane symmetry (i.e., the interaction of the z components of the spins is smaller than the one between the other components) exhibit a “topo-

logical” phase transition, related to the unbinding of vortex-antivortex pairs above a critical temperature T_{KT} , which can be observed only in 2D systems.⁷⁻⁹ Vortices are topological, nonlinear excitations characterized by a charge q . The impact of vortex-antivortex pairs below T_{KT} on the spin dynamics, as measured, e.g., by dynamical correlation functions, leads only to a renormalization of the spin wave peak.¹⁰ Above the transition temperature, however, the unbound moving vortices contribute to an additional central peak which has been observed both in computer simulations¹¹ and neutron scattering experiments on quasi-2D materials.¹² Analytic calculations by Mertens *et al.*¹³ predicted a quadratic Lorentzian shape of this central peak. In this approach the free vortices were considered to move ballistically with a Boltzmann velocity distribution characterized by an average thermal speed v_{rms} . The thermal speed was estimated by Huber¹⁴ from a velocity autocorrelation function based on a vortex equation of motion which was derived by Thiele¹⁵ using a collective-variable approach for localized structures in magnets. This calculation of v_{rms} , however, did not take into account the presence of different vortex structures for different strengths of the easy-plane anisotropy. Moreover, Thiele’s approach is for a single, well-localized excitation only, while its interactions with other excitations are treated through an external force term.

Vortices, however, have an infinitely extended static in-plane structure which also results in an extended perturbation of the static out-of-plane structure in the case of finite velocity. Though the superposition of the static in-plane structure of two vortices can be represented as a central force between their centers,⁷ this is no longer true for the superposition of their velocity-induced out-

of-plane structures. These corrections to the static vortex structure show up in the calculation of the mass and the gyro tensor of the Thiele equation and suggest that the single-vortex approach is no longer sufficient for an understanding of many-vortex dynamics. For finite temperatures the vortex size becomes finite due to screening¹⁶ (i.e., its structure is now localized), and a collective-variable approach seems to be appropriate to construct equations of motions for the vortex dynamics. However, as long as vortex radii are not much smaller than their average separations we still have to include the effects of the overlapping fields in understanding the many-vortex dynamics.

We introduce here a collective variable approach for N nonlinear excitations in magnetic systems. We derive N coupled equations of motion, each one of them similar to the original Thiele equation, but with additional inertial terms, resulting from an explicit dependence of the microscopic spin field on the vortex velocities. We then consider explicitly vortices in 2D easy-plane ferromagnets, which, for small anisotropies, already have statically a well-pronounced out-of-plane structure. Hence, each of them is characterized by two independent “charges,” namely its vorticity q and the sign of its static out-of-plane component p . We use approximate solutions¹⁷ to calculate the mass and gyro tensors of this system, which now become functions of the mutual vortex distance. The discussion of the dynamics becomes simplest for two vortices: they either rotate around each other ($q^1 p^1 = q^2 p^2$), or they move parallel to each other ($q^1 p^1 = -q^2 p^2$), with an additional small cyclotronlike oscillation on top of these trajectories. Due to the two-vortex corrections of the mass and gyro tensors this dynamic is now determined by two different masses which influence the amplitudes and frequencies differently for the various cases. This is in contrast to the one-vortex calculations, where one expects only one vortex mass. Comparison with numerical two-vortex simulations show good qualitative agreement with most of our analytic predictions. However, because we necessarily performed the simulations on a finite lattice at zero temperature, we also find an influence of the boundaries on the vortex parameters, which in some cases, is quite strong.

The paper is organized as follows: In Sec. II, we will briefly review the original approach of Thiele which led to an equation of motion for a single vortex. We also include a short discussion of a generalization of this ansatz including inertial effects which finally lead to a vortex mass. In Sec. III, we generalize the Thiele ansatz to a set of N localized magnetic structures. An application of these results to vortices in easy-plane Heisenberg ferromagnets is demonstrated in Sec. IV. In Sec. V, we discuss the special case of just two vortices, and briefly compare our analytic results with numerical simulations. Section VI contains a short summary.

II. SINGLE-VORTEX EQUATION OF MOTION

We will consider here magnetic systems which are described by the Landau-Lifshitz equation (LLE) with an additional Gilbert damping term

$$\dot{\mathbf{S}} = \mathbf{S} \times \left(-\frac{\delta \mathcal{H}}{\delta \mathbf{S}} \right) - \tilde{\alpha} \mathbf{S} \times \dot{\mathbf{S}}. \quad (1)$$

\mathbf{S} is a classical magnetization vector in units of \hbar , \mathcal{H} is the energy of the system, and $\tilde{\alpha}$ is a measure of the strength of the damping term. Equation (1) preserves the length of the spins, hence we can parametrize the vector $\mathbf{S}(\mathbf{r})$ with two canonically conjugated fields, the in-plane angle $\phi(\mathbf{r})$, and the z component of the spin field $m(\mathbf{r}) \equiv S_z(\mathbf{r}) = S \sin \theta(\mathbf{r})$ with the out-of-plane angle $\theta(\mathbf{r})$:

$$\mathbf{S} = (\sqrt{S^2 - m^2} \cos \phi, \sqrt{S^2 - m^2} \sin \phi, m). \quad (2)$$

Starting from Eq. (1) Thiele¹⁵ has derived an equation of motion for a single, well-localized excitation with center position $\mathbf{X}(t)$ under the assumption of steady-state motion [i.e., $\mathbf{S}(\mathbf{r}, t) = \mathbf{S}[\mathbf{r} - \mathbf{X}(t)]$ and $\dot{\mathbf{X}} = \text{const}$]; we refer to this as the Thiele-equation (TE)

$$\mathbf{F} + \mathbf{g} \times \dot{\mathbf{X}} - \mathbf{D} \dot{\mathbf{X}} = 0, \quad (3)$$

where, for a 2D system,

$$\mathbf{F} = - \int d^2 r \nabla \hat{\mathcal{H}}, \quad (4a)$$

$$\mathbf{g} = \int d^2 r \nabla \phi \times \nabla m, \quad (4b)$$

$$\mathbf{D} = \tilde{\alpha} \int d^2 r \left\{ \frac{\nabla m \nabla m}{S^2 - m^2} + (S^2 - m^2) \nabla \phi \nabla \phi \right\}. \quad (4c)$$

\mathbf{F} is the net force on an excitation due to other excitations or external fields, $\hat{\mathcal{H}}$ is the energy density of the system, the gyrovectore \mathbf{g} is a topological invariant for the system as a whole, \mathbf{D} is the damping matrix, and ∇ is the gradient with respect to \mathbf{r} .

This approach was applied to single vortices in 2D easy-plane Heisenberg ferromagnets^{14,18} (HFM) with Hamiltonian

$$\mathcal{H} = \frac{J}{2} \int d^2 r \{ (\nabla \mathbf{S})^2 + 4\delta S_z^2 - \delta (\nabla S_z)^2 \} \quad (5)$$

(which is the continuum limit of the discrete model $\mathcal{H} = \sum_{\langle ij \rangle} [\mathbf{S}_i \mathbf{S}_j - \delta (S_z)_i (S_z)_j]$). The material parameter $0 < \delta \leq 1$ measures the anisotropy of the system with the two limiting cases $\delta = 0$ and $\delta = 1$ corresponding to the isotropic and planar Heisenberg models, respectively. Depending on δ there exist two types of stable vortex structures with distinct dynamics.^{17,19} For $\delta \geq \delta_c$ (≈ 0.29 on a square lattice) static vortices are purely in plane; for $\delta < \delta_c$ they also have a well-localized out-of-plane structure around their core. The size of this S^z component increases with decreasing δ , allowing for a continuous crossover to the isotropic Heisenberg limit, where the topological excitations are instantons and merons rather than vortices. A single static vortex at position $\mathbf{X}(t) = (X_1, X_2)$ (lower indices denote the vector components) has the form¹⁷

$$\phi_s(\mathbf{r} - \mathbf{X}) = q \arctan \frac{y - X_2}{x - X_1}, \quad (6)$$

$$m_s(\mathbf{r} - \mathbf{X}) = pm_0(|\mathbf{r} - \mathbf{X}|),$$

where $m_0(r)$ has a well-localized peak at $r = 0$, while its large- r limit is given by

$$m_0(r) \approx \sqrt{\frac{r_v}{r}} e^{-r/r_v} \quad (7)$$

with the vortex core radius $r_v = \frac{1}{2} \sqrt{\frac{1-\delta}{\delta}}$ [Fig. 1(a)]. For $\delta < \delta_c$ the so-called polarization $p = \pm 1$ denotes the sign of the static out-of-plane structure, while $p = 0$ for $\delta > \delta_c$. This static structure becomes distorted when the vortex is moving and in lowest order in velocity this change in its shape is¹⁷

$$\phi_v(\mathbf{r} - \mathbf{X}; \dot{\mathbf{X}}) = p \tilde{\phi}(|\mathbf{r} - \mathbf{X}|) \frac{(\mathbf{r} - \mathbf{X}) \cdot \dot{\mathbf{X}}}{|\mathbf{r} - \mathbf{X}|}, \quad (8a)$$

$$\tilde{\phi}(r) = K m_0(r),$$

$$m_v(\mathbf{r} - \mathbf{X}; \dot{\mathbf{X}}) = qC \tilde{m}(\mathbf{r} - \mathbf{X}) \frac{[(\mathbf{r} - \mathbf{X}) \times \dot{\mathbf{X}}] \cdot \mathbf{e}_z}{|\mathbf{r} - \mathbf{X}|^2}, \quad (8b)$$

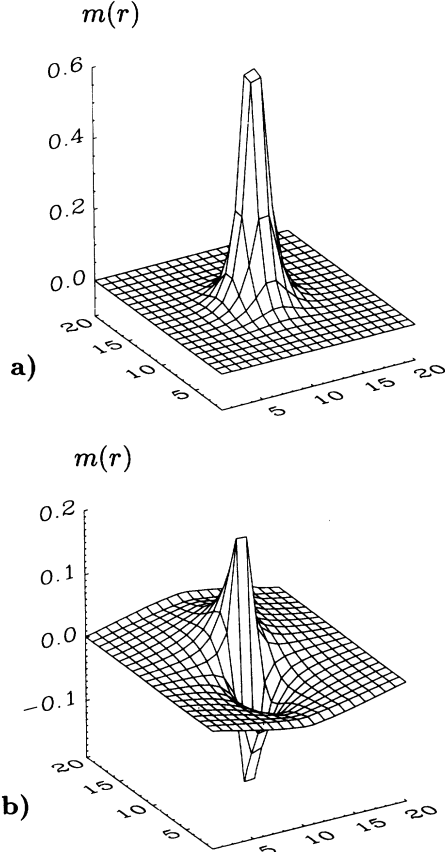


FIG. 1. Out-of-plane fields of single vortices: (a) static structure for $\delta = 0.2$; (b) velocity-induced structure for a vortex moving in the x direction with velocity $v = 0.1(aJS)$ and $\delta = 1$.

with $K = \frac{r_v}{JS}$ and $C = (4\delta JS^2)^{-1}$. The velocity-induced change in the in-plane field is as equally localized as the static out-of-plane structure. The dynamic out-of-plane structure, on the other hand, decays only as $\frac{1}{r}$ [i.e., $\tilde{m}(r \gg 1) \cong 1$]. The deviation of this asymptotic shape of $m_v(\mathbf{r})$ for small distances from the vortex core is described by $\tilde{m}(r)$. Since the main part of the angular anisotropy is evidently covered by the cross product $(\mathbf{r} - \mathbf{X}) \times \dot{\mathbf{X}}$, as can be seen from Fig. 1(b), we will simplify our following calculations by assuming \tilde{m} to be a function of the radial coordinate r alone. This angular dependence of $m_v(\mathbf{r})$ is not only observed for a single moving vortex. Simulations of vortex pairs exhibit an angular dependence of the spin field which, in first and dominant order, can be well described by a linear superposition of single-vortex contributions. Hence, we are confident that a use of this symmetry in the two-vortex integrals in Sec. IV is appropriate.

Inserting (6) and (8a) into (4) yields an equation of motion which can quite successfully describe the vortex dynamics with (sufficiently strong) damping, as was shown explicitly through numerical simulations of the LLE for two vortices.¹⁹ However, if we set the damping parameter $\tilde{\alpha} = 0$, the TE no longer makes sense for in-plane vortices ($\delta > \delta_c$), because here the gyro vector vanishes and \mathbf{F} need not be zero. It is interesting to consider why the TE is invalid for in-plane vortices. The difficulty stems from the fact that the z component is zero for the static vortex, and then changes appreciably (in a relative sense) with velocity. Thus, the basic assumption of a fixed vortex shape that simply makes a rigid translation is strongly violated. This problem is smaller for the out-of-plane vortices because the velocity-dependent changes in m are small compared to the static out-of-plane structure. Nevertheless, the TE cannot explain why out-of-plane vortices perform small oscillations around their mean trajectories as observed in computer simulations with small or zero damping (see below).

Wysin *et al.*²⁰ therefore proposed a more general ansatz for the spin field where the time dependence enters explicitly not only through the vortex position, but also through its velocity:

$$\mathbf{S} = \mathbf{S}[\mathbf{r} - \mathbf{X}(t), \dot{\mathbf{X}}(t)]. \quad (9)$$

Inserting (9) into (1) and following the procedure of Thiele leads to the generalized Thiele equation (GTE)

$$\mathbf{F} + \mathbf{g} \times \dot{\mathbf{X}} - \mathbf{D}\dot{\mathbf{X}} = \mathbf{M}\ddot{\mathbf{X}}, \quad (10)$$

where \mathbf{F} , \mathbf{g} , and \mathbf{D} are defined in (4), while \mathbf{M} is an effective mass tensor with components

$$\mathbf{M}_{ij} = - \int d^2r \left(\frac{\partial \phi}{\partial x_i} \frac{\partial m}{\partial \dot{X}_j} - \frac{\partial \phi}{\partial \dot{X}_j} \frac{\partial m}{\partial x_i} \right). \quad (11)$$

Because of the dependence of the fields on $\mathbf{r} - \mathbf{X}$ we can rewrite the gradients in \mathbf{M} , \mathbf{D} , and \mathbf{g} into gradients with respect to $\dot{\mathbf{X}}$ ($\frac{\partial}{\partial \mathbf{r}} \rightarrow -\frac{\partial}{\partial \dot{\mathbf{X}}}$). This form of the mass and damping tensors and the gyro vector (i.e., a pure dependence on gradients of the fields with respect to the collective variable $\dot{\mathbf{X}}$) can also be obtained by using the more

generalized ansatz $\mathbf{S} = \mathbf{S}(\mathbf{r}; \mathbf{X}, \dot{\mathbf{X}})$, if one immediately uses the gradient with respect to \mathbf{X} in the Thiele ansatz. This fact will allow us to generalize Thiele's ansatz to more than one excitation (see Sec. III).

For a single-vortex system the mass tensor is diagonal: $M_{ij} = M_0 \delta_{ij}$ with M_0 given in Eq. (19a). Since we do not know the exact form of the field $m(r)$, we can try to determine the mass through numerical simulations of the complete spin system (the gyro vector can be easily evaluated analytically, giving $\mathbf{g} = 2\pi q p \mathbf{e}_z$). Without an external field the force \mathbf{F} is zero and the vortex is expected to perform a circular motion with angular frequency $\omega_c = \frac{|\mathbf{g}|}{M_0}$. However, this is difficult to test by direct numerical simulations: Because the LLE (1) is of first order in time we need the exact shape of a moving vortex as an initial condition. But this shape is known only in the continuum limit and only far away from the vortex center. The situation is more favorable for a two-vortex system, where the two vortices drive each other, leading to a steady-state motion after a short transient time of adaption to the lattice. Because of the extended structure of the vortices their mutual interaction is not only described by a central force,⁷ but also by a renormalized mass tensor and gyro vector. A generalization of the single-structure collective variable ansatz to many excitations will be performed in the following section.

III. GENERALIZATION TO N LOCALIZED EXCITATIONS

The equation of motion derived in the previous section describes only the dynamics of a single localized structure, though the influence of other similar excitations can be included in the external force term. With this strategy, however, one will neglect important information about the parameters given as integrals over the spin field (i.e., the gyro and mass tensor). Especially, one would expect the appearance of two-center integrals representing the mutual influence of different excitations on each other. To include all these effects for a system with N well-localized excitations we will in this section generalize the modified Thiele ansatz (9) further, supposing an explicit dependence of the spin field on all the positions $\mathbf{X}^\alpha(t)$ and velocities $\dot{\mathbf{X}}^\alpha(t)$, $\alpha = 1, \dots, N$:

$$\mathbf{S}(\mathbf{r}, t) = \mathbf{S}(\mathbf{r}; \mathbf{X}^1, \dots, \mathbf{X}^N; \dot{\mathbf{X}}^1, \dots, \dot{\mathbf{X}}^N) \quad (12)$$

(the upper indices always denote the different excitations). To derive equations of motion for the collective variables \mathbf{X}^α we will make use of the canonical equations of motion for the total time derivatives of the fields ϕ and m :

$$\frac{d\phi}{dt} = \sum_{j,\beta} \dot{X}_j^\beta \frac{\partial \phi}{\partial X_j^\beta} + \sum_{j,\beta} \ddot{X}_j^\beta \frac{\partial \phi}{\partial \dot{X}_j^\beta} = \frac{\delta \mathcal{H}}{\delta m}, \quad (13a)$$

$$\frac{dm}{dt} = \sum_{j,\beta} \dot{X}_j^\beta \frac{\partial m}{\partial X_j^\beta} + \sum_{j,\beta} \ddot{X}_j^\beta \frac{\partial m}{\partial \dot{X}_j^\beta} = -\frac{\delta \mathcal{H}}{\delta \phi}. \quad (13b)$$

Multiplying (13a) by $\frac{\partial m}{\partial X_i^\alpha}$ and (13b) by $-\frac{\partial \phi}{\partial X_i^\alpha}$, adding the two resulting equations, and integrating over \mathbf{r} leads to N coupled equations of motion for the N collective variables $\mathbf{X}^\alpha(t)$:

$$\sum_{\beta=1}^N \left\{ \mathbf{M}^{\alpha\beta} \ddot{\mathbf{X}}^\beta + \mathbf{G}^{\alpha\beta} \dot{\mathbf{X}}^\beta \right\} = -\nabla^\alpha E, \quad \alpha = 1, \dots, N, \quad (14)$$

which are all of GTE-type. The mass ($\mathbf{M}^{\alpha\beta}$) and gyro tensors ($\mathbf{G}^{\alpha\beta}$) are defined as

$$\mathbf{M}_{ij}^{\alpha\beta} = \int d^2r \left\{ \frac{\partial \phi}{\partial X_i^\alpha} \frac{\partial m}{\partial X_j^\beta} - \frac{\partial \phi}{\partial X_j^\beta} \frac{\partial m}{\partial X_i^\alpha} \right\}, \quad (15a)$$

$$\mathbf{G}_{ij}^{\alpha\beta} = \int d^2r \left\{ \frac{\partial \phi}{\partial X_i^\alpha} \frac{\partial m}{\partial X_j^\beta} - \frac{\partial \phi}{\partial X_j^\beta} \frac{\partial m}{\partial X_i^\alpha} \right\}, \quad (15b)$$

i.e., there exist, as expected, single- and two-excitation contributions. ∇^α is the gradient with respect to \mathbf{X}^α and E is the energy of the system.

The above derivation of the equation of motion is purely Hamiltonian. Damping can be included following a similar scheme as Thiele,¹⁵ which leads to an additional term $D_{ij}^{\alpha\beta} \dot{\mathbf{X}}_j^\beta$ on the left-hand side of Eq. (14) with

$$\mathbf{D}_{ij}^{\alpha\beta} = \frac{\tilde{\alpha}}{S^2} \int d^2r \left\{ \frac{\partial \mathbf{S}}{\partial \mathbf{X}_i^\alpha} \cdot \frac{\partial \mathbf{S}}{\partial \mathbf{X}_j^\beta} \right\}. \quad (16)$$

IV. APPLICATION TO AN N -VORTEX SYSTEM

In the following we will consider explicitly a classical Heisenberg FM with weak easy-plane anisotropy ($\delta \lesssim 0.29$), where the localized excitations are out-of-plane vortices as described in Eq. (6). This case is particularly interesting, not only because here the gyro tensors are nonzero, but also because discreteness effects are very small,¹⁹ so that we can directly compare our analytical calculations to numerical simulations without the need of adding a (phenomenological) pinning potential to the equations of motion (cf. Sec. V). Moreover, we will focus our study here on systems with no damping term (i.e., $\tilde{\alpha} = 0$). This will allow us to obtain a clearer picture of the effects of the inertial term on the vortex dynamics and will emphasize the differences with overdamped dynamics which has been studied earlier.¹⁹

We will study systems of unbound vortices, without taking into account interactions with spin waves or tightly bound vortex-antivortex pairs which can be created spontaneously for finite temperatures. To allow for an analytic calculation of the mass and gyro tensors we will restrict ourselves to systems where the vortices are well separated, i.e., where their mutual distances are larger than twice the radius r_v of the static out-of-plane structures. In this case it is justified to construct the spin field as a linear superposition of single-vortex solutions (6), since the static in-plane field is a solution of

the Laplace equation, while the other fields are either well localized with vanishing contributions at the centers of neighboring vortices, or they are very small beyond a radius r_v .

The energy of such an N -vortex system is given by⁷

$$E = - \sum_{\alpha > \beta} k q^\alpha q^\beta \ln |\mathbf{X}^\alpha - \mathbf{X}^\beta| + E_c, \quad k = 2\pi J S^2, \quad (17)$$

from which we derive

$$\nabla^\alpha E = -k q^\alpha \sum_{\beta \neq \alpha} q^\beta \frac{\mathbf{X}^\alpha - \mathbf{X}^\beta}{|\mathbf{X}^\alpha - \mathbf{X}^\beta|^2}. \quad (18)$$

E_c contains the contributions from the static out-of-plane vortex structures, which are independent of the vortex position due to their localized shape, and the velocity-dependent corrections of the vortex shapes to the total energy are quadratic in the velocity. Because we restrict ourselves to well-separated vortices their velocities are small and we will neglect these terms of second order in the vortex velocities.

For the calculation of the leading contribution to the gyro tensors it is sufficient to consider only the static parts of the ϕ and S_z fields, while for the mass tensors we only need the static part of the ϕ and the velocity-induced part of the S_z field (the velocity-induced part of the ϕ field is already exponentially small). If we assume that $\tilde{m}(r)$ depends on the radial coordinate r only [which seems to be justified by comparing with the numerically obtained \tilde{m} field for $\delta = 0$ in Fig. 1(b)], then we can perform all of the angle integrations exactly. These tell

$$\mathbf{M}_{ij}^{\alpha\beta} = q^\alpha q^\beta \begin{pmatrix} \mathbf{M}_0 - \chi(d^{\alpha\beta}) + \psi(d^{\alpha\beta}) & 0 \\ 0 & \mathbf{M}_0 - \chi(d^{\alpha\beta}) - \psi(d^{\alpha\beta}) \end{pmatrix}, \quad \alpha \neq \beta, \quad (20)$$

with the abbreviations $d^{\alpha\beta} = |\mathbf{X}^\alpha - \mathbf{X}^\beta|$,

$$\psi(d^{\alpha\beta}) = \frac{\pi C}{(d^{\alpha\beta})^2} \int_{a_0}^L dr r \tilde{m}(r), \quad (21)$$

and

$$\chi(d^{\alpha\beta}) = \pi C \int_{a_0}^L dr \frac{\tilde{m}(r)}{r} + \pi K \int_{a_0}^L dr r m_0(r) m_0'(r). \quad (22)$$

With the help of the operator $\hat{\mathbf{P}}_{ij}^{\alpha\beta}$, which projects out the component parallel to $\mathbf{X}^\alpha - \mathbf{X}^\beta$ when applied to an arbitrary vector, we can rewrite (20) in the coordinate independent form

$$\mathbf{M}_{ij}^{\alpha\beta} = q^\alpha q^\beta \left\{ (\mathbf{M}_0 - \psi(d^{\alpha\beta}) + \chi(d^{\alpha\beta}) (2\hat{\mathbf{P}}_{ij}^{\alpha\beta} - \delta_{ij})) \right\}. \quad (23)$$

All the mass tensors depend on \mathbf{M}_0 which increases logarithmically with L , if we insert the asymptotic single vortex solution for a slowly moving vortex [Eqs. (6) and (8a)].

us which of the matrix elements are zero and which are not.

For the one-vortex mass and gyro tensor we obtain the same result as Huber¹⁴ and Pokrovsky,¹⁸ however, with an additional contribution from the dynamically distorted in-plane field, namely

$$\mathbf{M}_{ij}^{\alpha\alpha} = \mathbf{M}_0 \delta_{ij}, \quad (19a)$$

$$\mathbf{M}_0 = \pi C \int_{a_0}^L dr \frac{\tilde{m}(r)}{r} + \pi K \int_{a_0}^L dr r m_0(r) m_0'(r),$$

$$\mathbf{G}_{ij}^{\alpha\alpha} = 2\pi q^\alpha p^\alpha \epsilon_{ij}, \quad (19b)$$

δ_{ij} and ϵ_{ij} are the 2D unit and completely antisymmetric tensors, respectively, a_0 is a lower cutoff of the order of a lattice constant, and L is the system size. (In the analytic calculations L is the radius of a circular symmetric plane, hence, in our numerical simulations on a square lattice we choose L to be half of the linear dimension of the system.)

The two-vortex contributions, however, depend on the choice of the coordinate system and are only diagonal for a system with axes parallel and perpendicular to the line connecting the two vortices under consideration. (In general these coordinate systems clearly do not coincide for different pairs of the same system.) In the coordinate system with the first axis parallel to $\mathbf{X}^\alpha - \mathbf{X}^\beta$, the second perpendicular to it (which we will refer to as the main frame system of the two vortices under consideration), we find for the mass tensors

For the two-vortex gyro tensors it is convenient to discuss the cases $q^\alpha p^\beta = q^\beta p^\alpha$ (i.e., $\mathbf{G}_{ij}^{\alpha\alpha} = \mathbf{G}_{ij}^{\beta\beta}$) and $q^\alpha p^\beta = -q^\beta p^\alpha$ (i.e., $\mathbf{G}_{ij}^{\alpha\alpha} = -\mathbf{G}_{ij}^{\beta\beta}$) separately. In the first case the gyro tensors are independent on the underlying coordinate system and we obtain the completely antisymmetric matrix

$$\mathbf{G}_{ij}^{\alpha\beta} = 2\pi q^\alpha p^\beta [m_0(d^{\alpha\beta}) - m_0(L)] \epsilon_{ij}, \quad \alpha \neq \beta. \quad (24)$$

Since we consider only mutual vortex distances $d^{\alpha\beta} > r_v$, these contributions are exponentially small [cf. Eq. (7)]. For $q^\alpha p^\beta = -q^\beta p^\alpha$ we obtain for the gyro tensors in the main frame system (cf. the discussion of the mass tensor)

$$\mathbf{G}_{ij}^{\alpha\beta} = 2\pi q^\alpha p^\beta \zeta(d^{\alpha\beta}) \begin{pmatrix} 0 & 1 \\ -1 & 0 \end{pmatrix}, \quad (25)$$

$$\zeta(d^{\alpha\beta}) = -\frac{1}{(d^{\alpha\beta})^2} \int_{a_0}^L dr r^2 m_0'(r),$$

or in general

$$\mathbf{G}_{ij}^{\alpha\beta} = 2\pi q^\alpha p^\beta \zeta(d^{\alpha\beta}) \epsilon_{ik} (2\hat{\mathbf{S}}_{kj}^{\alpha\beta} - \delta_{kj}), \quad \alpha \neq \beta, \quad (26)$$

where the operator $\hat{\mathbf{S}}_{kj}^{\alpha\beta}$ projects out the component perpendicular to $\mathbf{X}^\alpha - \mathbf{X}^\beta$ when applied to an arbitrary vector. In this case the components of $\mathbf{G}^{\alpha\beta}$ decay as $(d^{\alpha\beta})^{-2}$.

V. COMPARISON WITH NUMERICAL SIMULATIONS OF TWO-VORTEX SYSTEMS

We will now apply our ansatz to two-vortex systems and compare the analytical results to numerical simulations of the complete spin system. Because we have two “quantum numbers” per vortex, namely its vorticity q and the sign of its out-of-plane structure p , we have to distinguish between four physically different cases, when considering two pairs. This is different from the vortex-pair dynamics in other systems, like, e.g., incompressible fluids, where each vortex is characterized by a single “quantum number,” leading to only two different scenarios in a two-vortex system.

A. The equations of motion

For a two-vortex system it is more convenient to rewrite the equations of motion (14) in center-of-mass (cms) $\mathbf{C} = \frac{1}{2}(\mathbf{X}^1 + \mathbf{X}^2)$ and relative coordinate $\mathbf{Y} = \mathbf{X}^1 - \mathbf{X}^2$

$$\bar{\mathbf{M}}\ddot{\mathbf{C}} + \tilde{\mathbf{M}}\ddot{\mathbf{Y}} + \bar{\mathbf{G}}^1\dot{\mathbf{C}} + \tilde{\mathbf{G}}^1\dot{\mathbf{Y}} = \frac{kq^1q^2}{Y^2}\mathbf{Y}, \quad (27a)$$

$$\bar{\mathbf{M}}\ddot{\mathbf{C}} - \tilde{\mathbf{M}}\ddot{\mathbf{Y}} + \bar{\mathbf{G}}^2u\dot{\mathbf{C}} - \tilde{\mathbf{G}}^2\dot{\mathbf{Y}} = -\frac{kq^1q^2}{Y^2}\mathbf{Y}. \quad (27b)$$

(For a derivation of the above equations and the definition of the consequent mass and gyro tensors see the Appendix.) In a system with the first axis parallel, the second perpendicular, to \mathbf{Y} , the mass tensors become diagonal

$$\bar{\mathbf{M}} = \begin{pmatrix} \bar{M}_1 & 0 \\ 0 & \bar{M}_2 \end{pmatrix}, \quad \tilde{\mathbf{M}} = \frac{1}{2} \begin{pmatrix} \tilde{M}_1 & 0 \\ 0 & \tilde{M}_2 \end{pmatrix}, \quad (28)$$

with

$$\bar{M}_1 = (1 + q^1q^2)\mathbf{M}_0 - q^1q^2(\chi - \psi), \quad (29a)$$

$$\bar{M}_2 = (1 + q^1q^2)\mathbf{M}_0 - q^1q^2(\chi + \psi), \quad (29b)$$

$$\tilde{M}_1 = (1 - q^1q^2)\mathbf{M}_0 + q^1q^2(\chi - \psi), \quad (29c)$$

$$\tilde{M}_2 = (1 - q^1q^2)\mathbf{M}_0 + q^1q^2(\chi + \psi). \quad (29d)$$

These are now no longer single-vortex masses, but $\bar{\mathbf{M}}$ can be considered as total mass of the two-vortex system, \tilde{M}_1 as the reduced mass.

The dependence of the gyro tensors on the products $q^\alpha p^\beta$ suggests that we distinguish the cases $q^1p^2 = q^2p^1$ and $q^1p^2 = -q^2p^1$.

(a) $q^1p^2 = q^2p^1$: (vortex rotation). For this case we find for the gyro tensors

$$\bar{\mathbf{G}}^1 = \bar{\mathbf{G}}^2 \equiv \bar{\mathbf{G}} \quad \text{and} \quad \tilde{\mathbf{G}}^1 = \tilde{\mathbf{G}}^2 \equiv \tilde{\mathbf{G}}. \quad (30)$$

Equation (27) can only be satisfied if \mathbf{C} is a constant (which, without loss of generality, can be set zero). Using Eqs. (A2) and (24) we obtain a completely antisymmetric gyro tensor $\tilde{\mathbf{G}}_{ij}^1 = \pi q^1(p^1 - p^2)\epsilon_{ij} \equiv \frac{1}{2}q^1p^1G\epsilon_{ij}$, $\mu = m_0(d) - m_0(L)$, which allows us to rewrite the product $\tilde{\mathbf{g}}\dot{\mathbf{Y}}$ as a cross product $\dot{\mathbf{Y}} \times \mathbf{g}$ with the gyro vector $\mathbf{g} = G\mathbf{e}_z$. This leads finally to the single equation of motion

$$\tilde{\mathbf{M}}\ddot{\mathbf{Y}} - \mathbf{g} \times \dot{\mathbf{Y}} = 2\frac{kq^1q^2}{Y^2}\mathbf{Y}. \quad (31)$$

Though (31) looks similar to Eq. (10) for a single vortex, there are two important differences: (i) the mass is now represented by a tensor leading to two different masses for the two main frame directions, and (ii) the masses depend on the mutual vortex distance (the dependence of G on the mutual distance is exponentially small and will be neglected in the following discussion). A particular solution of (31) is a rotation of the two vortices around each other at a distance d with angular velocity

$$\omega_0 = \frac{1}{2}\frac{G}{\tilde{M}_1} \left\{ 1 - \sqrt{1 - \frac{4q^1q^2}{\pi} \frac{\tilde{M}_1}{d^2}} \right\} \quad (32)$$

and an additional cyclotronlike oscillation around this trajectory. Using the abbreviations $y = \pi R_0^2/\tilde{M}_1$ and $R_0 = d/2$, we can rewrite Eq. (32) as

$$\omega_0 R_0^2 = q^1p^1y \left\{ 1 - \sqrt{1 - \frac{q^1q^2}{y}} \right\}, \quad (33)$$

which has for vanishing mass \tilde{M}_1 (i.e., $y \rightarrow \infty$) the expansion

$$\omega_0 R_0^2 = \frac{q^1p^1}{2} + \frac{q^2p^1}{8y} + o\left(\frac{1}{y^2}\right), \quad (34)$$

with the result of the original Thiele equation (without inertial force) as leading term. In the case of vortex-vortex rotation, where \tilde{M}_1 depends only on the difference of the distance-dependent functions χ and ψ , we expect only small deviations of $|\omega_0 R_0^2|$ from $\frac{1}{2}$.

If we assume that the amplitudes of the cyclotronlike oscillation are small compared to the radius R_0 of the main circular motion, then we can linearize the equation of motion (31) and obtain the solution

$$\mathbf{Y} = 2R\mathbf{e}_r = 2R(\cos\varphi\mathbf{e}_x, \sin\varphi\mathbf{e}_y) \quad (35)$$

with

$$R(t) = R_0 + r_0 \cos \omega t, \quad \varphi(t) = \omega_0 t + \varphi_0 \sin \omega t, \quad (36)$$

and

$$\omega^2 = \omega_c^2 \left\{ 1 - \left(2 \frac{\tilde{M}_2 + \tilde{M}_1}{\sqrt{\tilde{M}_1 \tilde{M}_2}} + R_0 \frac{\partial \ln \omega_0}{\partial R_0} \sqrt{\frac{\tilde{M}_2}{\tilde{M}_1}} \right) \frac{\omega_0}{\omega_c} + \left(4 + 2R_0 \frac{\partial \ln \omega_0}{\partial R_0} \right) \left(\frac{\omega_0}{\omega_c} \right)^2 \right\}, \quad (37)$$

where $\omega_c^2 = G^2 / \tilde{M}_1 \tilde{M}_2$. The amplitude ratio of this cyclotronlike oscillation in the R and φ directions, respectively, is

$$\frac{R_0 \varphi_0}{r_0} = \frac{G / \tilde{M}_2 - 2\omega_0}{\omega}, \quad (38)$$

which becomes proportional to the mass ratio $\sqrt{\tilde{M}_1 / \tilde{M}_2}$ for large mutual vortex distances d .

(b) $q^1 p^2 = -q^2 p^1$: (vortex translation). For this case we derive from Eqs. (26) and (A2) the gyro tensors

$$\bar{\mathbf{G}}^1 = -\bar{\mathbf{G}}^2 \equiv \bar{\mathbf{G}} = 2\pi q^1 \begin{pmatrix} 0 & p^1 + p^2 \zeta \\ -(p^1 - p^2 \zeta) & 0 \end{pmatrix}, \quad (39a)$$

$$\tilde{\mathbf{G}}^1 = -\tilde{\mathbf{G}}^2 \equiv \tilde{\mathbf{G}} = \pi q^1 \begin{pmatrix} 0 & p^1 - p^2 \zeta \\ -(p^1 + p^2 \zeta) & 0 \end{pmatrix}. \quad (39b)$$

The two resulting equations of motion (27) only have solutions for vectors \mathbf{r} and \mathbf{Y} which are perpendicular to each other. For example if we set $\mathbf{X}^1 = (x, y)$ and $\mathbf{X}^2 = (-x, y)$, we obtain the two equations of motion

$$\tilde{M}_1 \ddot{y} + g\dot{x} = \frac{kq^1 q^2}{2y}, \quad (40a)$$

$$\bar{M}_2 \ddot{x} - g\dot{y} = 0, \quad (40b)$$

with

$$g = 2\pi q^1 p^1 (1 + \hat{\zeta}) \quad \text{and} \quad \hat{\zeta} = p^1 p^2 \zeta. \quad (41)$$

A solution of (40) is a parallel motion of the two vortices perpendicular to their connecting line with a constant speed v_0 which is related to their mutual distance d by

$$v_0 d = \frac{k}{g} = \frac{q^1 q^2}{q^1 p^1 (1 + p^1 p^2 \zeta)}, \quad (42)$$

i.e., we expect $|v_0 d|$ to be larger than 1 for the vortex-vortex case ($q^1 q^2 = 1$, $p^1 p^2 = -1$) and smaller than 1 for the vortex-antivortex case ($q^1 q^2 = -1$, $p^1 p^2 = 1$), respectively. Since ζ is small and only weakly d dependent, these corrections to 1 should be small and almost constant.

There are again cyclotronlike oscillations possible. If we assume their amplitudes to be small compared to the

mutual vortex distance d , then we can linearize Eq. (40) and obtain the complete solution

$$x(t) = v_0 t + \xi_0 \cos \omega t, \quad y(t) = \frac{d}{2} + \eta_0 \sin \omega t, \quad (43)$$

with

$$\omega^2 = \frac{(2\pi)^2}{\tilde{M}_1 \tilde{M}_2} \left\{ (1 + \hat{\zeta})^2 + \frac{q^1 q^2 \tilde{M}_2}{\pi d^2} \frac{1 - \hat{\zeta}}{1 + \hat{\zeta}} \right\}. \quad (44)$$

The ratio of the amplitudes of the small oscillations is given here by

$$\left(\frac{\xi_0}{\eta_0} \right)^2 = \frac{\tilde{M}_2}{\tilde{M}_1} \left\{ 1 + \frac{q^1 q^2 \tilde{M}_2}{\pi d^2} \frac{1 - \hat{\zeta}}{(1 + \hat{\zeta})^3} \right\}. \quad (45)$$

In contrast to the previous case we have now masses of different origin present (\tilde{M}_2 corresponds to the cms motion, \tilde{M}_1 to the relative motion of the two vortices) which have different dependences on the system size [cf. (29)].

B. Comparison with numerical simulations

We will now compare these results to numerical simulations of the complete spin systems on finite lattices (50×50 and 84×84) which have been performed in the following way: we initialized the system by putting the linear superposition of two approximate static single-vortex solutions (6) onto the lattice, then we integrate the LL equation (1) using a fourth-order Runge-Kutta algorithm with time step $\Delta t = 0.04(JS)^{-1}$ and free boundary conditions. The vortices will adapt rather quickly to their final shape due to the finite discrete lattice by radiating spin waves. To eliminate these initially excited spin waves we start the integration with a finite Gilbert damping parameter $\tilde{\alpha} = 0.1$ for a time period of $t = 40 \dots 80(JS)^{-1}$, during which the vortices follow an additional inward ($q^1 q^2 = -1$) or outward ($q^1 q^2 = 1$) trajectory. After switching off the damping parameter we are able to observe vortex dynamics as predicted in Sec. V A. Because the vortices have at this time already acquired quite a large velocity component in the forward direction, the additional cyclotronlike oscillations are not expected to be very well pronounced. All our simulations were performed at zero temperatures, where the vortices fill out the complete system, independent of its size. We therefore will discuss the results only in a qualitative way, since we expect rather strong boundary effects on the absolute values of the parameters, especially, when they depend on the total size of the vortices. However, as will be shown now, these simulations are already sufficient to demonstrate the impact of the two-vortex contributions on the mass and gyro tensors, as predicted by our calculations.

Figures 2 and 3 show typical simulation results for the 4 different vortex pair configurations.

(a) Vortex-vortex rotation: Data for these cases is listed in Table I. Here, we obtain one of the two masses (\tilde{M}_1) by measuring the rotational frequency. \tilde{M}_1 and the

used values for the vorticity (q) and the sign of the out-of-plane structure (p) determine the deviation of the product $|\omega_0 R_0^2|$ from $\frac{1}{2}$ [Eq. (34)]. In the vortex-vortex case ($q^1 = p^1 = q^2 = p^2 = 1$) this correction is small, positive, and almost constant, corresponding to a small mass $\tilde{M}_1 \propto d^2$: this observation agrees qualitatively with our analytic result $\tilde{M}_1 = \chi - \psi$ [Eq. (29)], which should depend only on the mutual vortex distance d , but not on the dominant one-vortex contribution $\tilde{M}_0 \propto \ln L$ [Eq. (19a)]. On the other hand, for the vortex-antivortex case ($-q^1 = p^1 = q^2 = -p^2 = 1$), the observed mass is larger, and both strongly d and system size dependent, corresponding to our expectation that this mass is dominated by the \tilde{M}_0 term. For the rotational vortex motion we can determine the second mass \tilde{M}_2 directly by measuring the frequency of the cyclotronlike oscillation. In the case of vortex-antivortex pairs we clearly observe this additional frequency. Table I lists values of \tilde{M}_2 from these simulations. As expected from Eq. (29), these values are different from those of \tilde{M}_1 , though they should also depend on the total vortex size. The strong, but different dependence of the two masses on d and the system

size, especially the negative value of $\psi = \frac{1}{2}(\tilde{M}_1 - \tilde{M}_2)$ for small radii and the sharp decrease of \tilde{M}_2 with increasing d , seem to show the strong influence of the boundaries on the two-vortex parameters. In the case of vortex-vortex rotation we do not observe a clearly pronounced cyclotron oscillation. This is probably caused by small amplitudes and by a high frequency $\omega > \omega_0$, if $\tilde{M}_2 \approx \tilde{M}_1$.

(b) Vortex-vortex translation: Data for these cases is listed in Table II. Here, we also find an impact of the two-vortex contributions on the value of the gyro vector. These show up as corrections of the product $|v_0 d|$ from 1 [Eq. (42)], independent on whether we consider vortex-vortex ($q^1 = p^1 = q^2 = -p^2 = 1$) or vortex-antivortex ($-q^1 = p^1 = q^2 = p^2 = 1$) pairs. In the latter case the simulations show corrections to $|v_0 d|$, which are basically constant for a wide variety of different d 's for a given system size. For the vortex-vortex case these corrections show a dependence on the orientation of the cms direction of motion to the boundaries, emphasizing again the impact of the system size on the dynamic parameters. As in the rotational case we find clearly visible cyclotronlike oscillations only in one of the two possible cases, but

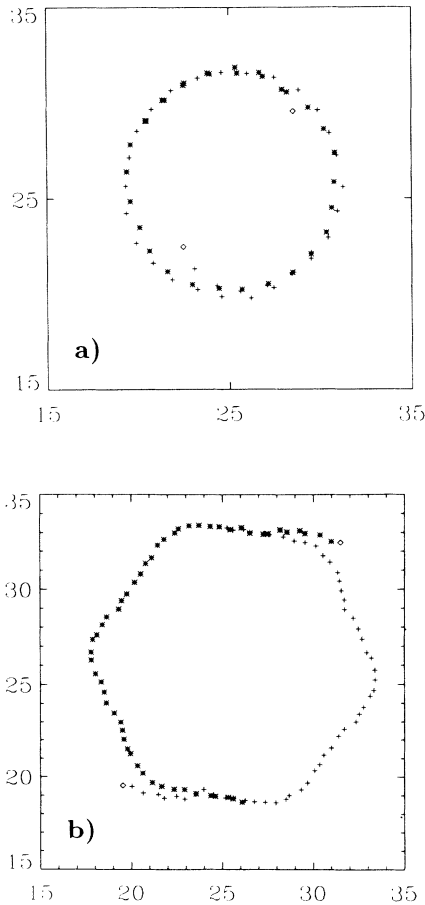


FIG. 2. Two-vortex simulation results on a 50×50 lattice with $\delta = 0.1$, showing rotation of the vortex pair around each other; (a) vortex-vortex pair ($q^1 = q^2 = p^1 = p^2 = +1$); (b) vortex-antivortex pair ($q^1 = -q^2 = -p^1 = p^2 = +1$); \diamond , initial positions; $+$, vortex 1; $*$, vortex two.

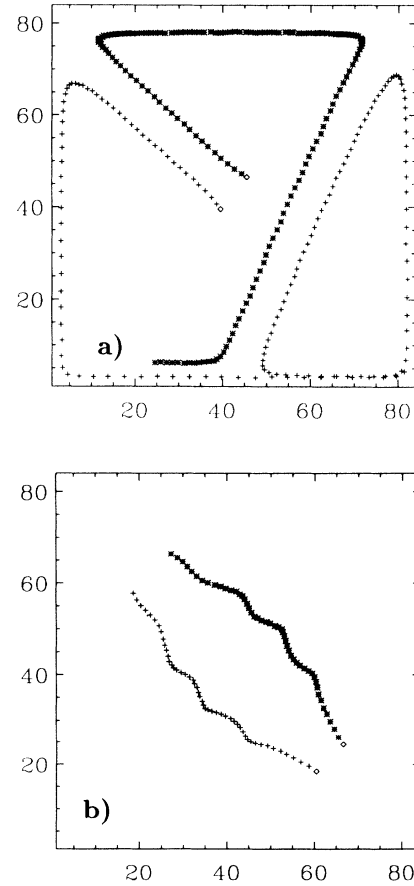


FIG. 3. Two-vortex simulation results on an 84×84 lattice with $\delta = 0.1$, showing translation of the vortex pair parallel each other; (a) vortex-antivortex pair ($q^1 = -q^2 = p^1 = p^2 = +1$); (b) vortex-vortex pair ($q^1 = q^2 = -p^1 = p^2 = +1$). Symbols denote the same as in Fig. 2.

TABLE I. Data for vortex pair rotation obtained from numerical simulations. Top: vortex-vortex pair ($q^1 q^2 = +1$); (b) vortex-antivortex pair ($q^1 q^2 = -1$); $y = \frac{\pi R_0^2}{\tilde{M}_1}$.

L	R_0	$ \omega_0 R_0^2 $	y	\tilde{M}_1
25	5.79	0.5266	5.21	20
25	8.69	0.5272	5.11	46
42	8.25	0.5140	9.44	23
42	12.51	0.5197	6.86	72

L	R_0	$ \omega_0 R_0^2 $	y	\tilde{M}_1	\tilde{M}_2	ψ
25	6.12	0.37	0.51	228	1764	-168
25	7.37	0.33	0.33	517	141	188
25	7.56	0.33	0.31	582	120	231
25	8.06	0.31	0.25	830	83	373
42	9.02	0.41	0.87	292	2507	-1108
42	10.60	0.38	0.61	579	327	126
42	11.83	0.36	0.44	922	161	416
42	12.15	0.34	0.37	1262	124	569

this time for vortex-vortex pairs. The reason for this observation is the fact that the dynamics depends here on two masses of different origin and size, leading to different amplitudes parallel and perpendicular to the cms motion [Eq. (45)]. For the vortex-vortex case the perpendicular amplitude (i.e., \tilde{M}_2) is large and the resulting oscillations are clearly visible [Fig. 3(b)], while for the vortex-antivortex case the parallel amplitude (i.e., \tilde{M}_1) is large. The latter is hard to observe by looking at the trajectories and can be seen in Fig. 3(a) only in the part of the trajectory parallel to the upper boundary. From this picture we can also learn that a single vortex moves along the boundary, as if there exists an image vortex just symmetrically outside the boundary with the proper q and p values, to force this motion. This picture is better, the closer a vortex is to its image vortex rather than to its partner within the system. This suggests that the

TABLE II. Data for vortex pair translation obtained from numerical simulations. Top: vortex-antivortex pair ($q^1 q^2 = +1$); bottom: vortex-vortex pair ($q^1 q^2 = -1$); (p), vortices move parallel to boundary; (d), vortices move parallel to the diagonal of the square lattice.

L	R_0	$ v_0 d $	ζ
25	5 ... 10	0.96	0.042
42	5 ... 15	0.92	0.087

L	R_0	$ v_0 d $	ζ
25	9.38 (p)	1.048	0.046
25	9.85 (p)	1.048	0.046
25	8.21 (d)	1.296	0.228
42	7.16 (p)	1.114	0.102
42	9.79 (p)	1.108	0.097
42	19.56 (p)	1.210	0.174
42	9.23 (d)	1.042	0.040
42	10.66 (d)	1.032	0.031
42	11.63 (d)	1.064	0.060

boundary effects can be understood in terms of one or more image vortices. In the translational case we need to measure both, the frequency and the amplitudes of the cyclotron oscillations, to obtain values for the masses. This will be done in a forthcoming paper, where we will also develop some methods to treat the boundary effects.

VI. CONCLUSIONS

We have presented a collective variable approach to a system of N well-localized excitations in a magnetic system. Generalizing earlier approaches which were restricted to single excitations only we obtained N coupled equations of motion of generalized Thiele form (i.e., with inertial, gyro, and external force terms). The tensors which describe the strength of the couplings between the excitations can be classified as (two-vortex) mass and gyro tensor, which now depend also on the mutual distances of the excitations.

As an example we applied this ansatz to an easy-plane Heisenberg ferromagnet where the localized excitations are vortices. Under the assumption that the vortices are all well separated from each other, we can calculate the mass and gyro tensors in the low velocity limit using the vortex shapes calculated by Gouvêa *et al.*¹⁷ By explicitly considering a two-vortex system, we discuss the possible vortex dynamics in detail and compare these results with numerical simulations of the complete spin system. From our theory we expect for these systems either a rotation of the vortices around each other, or a translation of them parallel to each other, and an additional cyclotronlike oscillation around these main trajectories. Two vortices are best described in cms and relative coordinates and the values of the corresponding masses can vary on a large scale depending on the vorticity and the sign of the out-of-plane structures of the participating vortices, and also the gyro tensor shows a distinct d dependence in the translational case. Our calculations predict correctly the deviations due to the two-vortex interactions from dynamical quantities, e.g., $|\omega_0 R_0^2|$ or $|v_0 d|$, as can be seen from the numerical simulations. However, since these simulations were performed on finite lattices at zero temperature, where the boundary effects have a strong influence on the absolute values of the masses, we cannot compare these values quantitatively with our analytic results for an infinite system. The effects of the boundary, which can in some cases be understood in terms of image vortices, will be discussed in a forthcoming paper.

ACKNOWLEDGMENTS

This work was supported by Deutsche Forschungsgemeinschaft (SFB 213, C19), NATO Collaborative Research Grant 0013/89, and by the United States department of Energy. We also thank M. Peyrard, Ecole Normale Supérieure de Lyon, for useful discussions.

APPENDIX: EQUATION OF MOTION
FOR TWO VORTICES

For a two-vortex system Eqs. (14) become

$$\begin{aligned} \mathbf{M}^{11}\ddot{\mathbf{X}}^1 + \mathbf{M}^{12}\ddot{\mathbf{X}}^2 + \mathbf{g}^{11}\dot{\mathbf{X}}^1 + \mathbf{g}^{12}\dot{\mathbf{X}}^2 \\ = kq^1q^2 \frac{\mathbf{X}^1 - \mathbf{X}^2}{|\mathbf{X}^1 - b\mathbf{X}z|^2}, \quad (\text{A1a}) \end{aligned}$$

$$\begin{aligned} \mathbf{M}^{21}\ddot{\mathbf{X}}^1 + \mathbf{M}^{22}\ddot{\mathbf{X}}^2 + \mathbf{g}^{21}\dot{\mathbf{X}}^1 + \mathbf{g}^{22}\dot{\mathbf{X}}^2 \\ = kq^1q^2 \frac{\mathbf{X}^2 - \mathbf{X}^1}{|\mathbf{X}^1 - b\mathbf{X}z|^2}. \quad (\text{A1b}) \end{aligned}$$

Introducing the cms and relative coordinates $\mathbf{C} = \frac{1}{2}(\mathbf{X}^1 + \mathbf{X}^2)$ and $\mathbf{Y} = \mathbf{X}^1 - \mathbf{X}^2$, respectively, allows us to rewrite (A1) as

$$\begin{aligned} (\mathbf{M}^{11} + \mathbf{M}^{12})\ddot{\mathbf{C}} + \frac{1}{2}(\mathbf{M}^{11} - \mathbf{M}^{12})\ddot{\mathbf{Y}} + (\mathbf{g}^{11} + \mathbf{g}^{12})\dot{\mathbf{C}} \\ + \frac{1}{2}(\mathbf{g}^{11} - \mathbf{g}^{12})\dot{\mathbf{Y}} = kq^1q^2 \frac{\mathbf{Y}}{Y^2}, \quad (\text{A2a}) \end{aligned}$$

$$\begin{aligned} (\mathbf{M}^{21} + \mathbf{M}^{22})\ddot{\mathbf{C}} + \frac{1}{2}(\mathbf{M}^{21} - \mathbf{M}^{22})\ddot{\mathbf{Y}} + (\mathbf{g}^{21} + \mathbf{g}^{22})\dot{\mathbf{C}}d \\ + \frac{1}{2}(\mathbf{g}^{21} - \mathbf{g}^{22})\dot{\mathbf{Y}} = -kq^1q^2 \frac{\mathbf{Y}}{Y^2}. \quad (\text{A2b}) \end{aligned}$$

Since the masses depend only on the vortex vorticities q^1 and q^2 , we can define the two new mass tensors

$$\bar{\mathbf{M}} = \mathbf{M}^{11} + \mathbf{M}^{12} = \mathbf{M}^{22} + \mathbf{M}^{21}, \quad (\text{A3a})$$

$$\tilde{\mathbf{M}} = \frac{1}{2}(\mathbf{M}^{11} - \mathbf{M}^{12}) = \frac{1}{2}(\mathbf{M}^{22} - \mathbf{M}^{21}). \quad (\text{A3b})$$

Similarly, we can define new gyro tensors, but here all the four different quantum numbers play a role. Thus, in general, we have to define four new gyrotensors:

$$\bar{\mathbf{G}}^i = \mathbf{G}^{ii} + \mathbf{G}^{ij}, \quad (\text{A4a})$$

$$\tilde{\mathbf{G}}^i = \frac{1}{2}(\mathbf{G}^{ii} - \mathbf{G}^{ij}), \quad i, j = 1, 2, \quad i \neq j, \quad (\text{A4b})$$

which, however, will be related to each other in the two special cases discussed in Sec. V. Inserting (A3) and (A4) into (A2) leads finally to Eq. (27).

- * Present address: Department of Physics, University of Toronto, Toronto, Ontario, Canada M5S 1A7.
- ¹ Permanent address: Department of Physics, Kansas State University, Manhattan, Kansas 66506.
- [†] Permanent address: Physics Institute, University of Bayreuth, 95440 Bayreuth, Germany.
- ¹ *Nonlinearity in Condensed Matter*, edited by A. R. Bishop, R. Ecke, and J. Gubernatis (Springer, Berlin, 1993).
- ² *Nonlinear Coherent Structures in Physics and Biology*, edited by K. H. Spatschek and F. G. Mertens (Plenum Press, New York, 1994).
- ³ A. M. Kosevich, *Sov. Phys. Usp.* **7**, 837 (1965).
- ⁴ R. Boesch, P. Stanicoff, and C. R. Willis, *Phys. Rev. B* **38**, 6713 (1988).
- ⁵ R. Boesch and C. R. Willis, *Phys. Rev. B* **42**, 6371 (1990).
- ⁶ *Magnetic Properties of Layered Transition Metal Compounds*, edited by L. J. de Jongh (Kluwer Academic Publisher, Dordrecht, 1990).
- ⁷ J. M. Kosterlitz and D. J. Thouless, *J. Phys. C* **6**, 1181 (1973).
- ⁸ J. M. Kosterlitz and D. J. Thouless, *J. Phys. C* **7**, 1046 (1974).

- ⁹ V. L. Berezinskii, *Sov. Phys. JETP* **34**, 610 (1972).
- ¹⁰ R. Côte and A. Griffin, *Phys. Rev. B* **34**, 6240 (1986).
- ¹¹ F. G. Mertens, A. R. Bishop, G. M. Wysin, and C. Kawabata, *Phys. Rev. B* **39**, 591 (1989).
- ¹² D. G. Wiesler, H. Zabel, and S. M. Shapiro, *Z. Phys. B* **93**, 277 (1994).
- ¹³ F. G. Mertens, A. R. Bishop, G. M. Wysin, and C. Kawabata, *Phys. Rev. Lett.* **59**, 117 (1987).
- ¹⁴ D. L. Huber, *Phys. Rev. B* **26**, 3758 (1982).
- ¹⁵ A. A. Thiele, *Phys. Rev. Lett.* **30**, 230 (1973).
- ¹⁶ P. Olsson, *Phys. Rev. B* **46**, 14598 (1992).
- ¹⁷ M. E. Gouvêa, G. M. Wysin, A. R. Bishop, and F. G. Mertens, *Phys. Rev. B* **39**, 11840 (1989).
- ¹⁸ V. L. Pokrovsky and D. V. Khveshchenko, *Sov. Low Temp. Phys.* **14**, 213 (1988).
- ¹⁹ A. R. Völkel, F. G. Mertens, A. R. Bishop, and G. M. Wysin, *Phys. Rev. B* **43**, 5992 (1991).
- ²⁰ G. M. Wysin, F. G. Mertens, A. R. Völkel, and A. R. Bishop, in *Nonlinear Coherent Structures in Physics and Biology*, edited by K. H. Spatschek and F. G. Mertens (Plenum Press, New York, 1994).